Engineered disulfides improve mechanical properties of recombinant spider silk

S. Grip,[1,2] J. Johansson,[1] and M. Hedhammar[1]*

[1]Department of Anatomy, Physiology and Biochemistry, Swedish University of Agricultural Sciences, The Biomedical Centre, Uppsala 751 23, Sweden

[2]Department of Biomedical Sciences and Veterinary Public health, Swedish University of Agricultural Sciences, Uppsala 75007, Sweden

Received 15 December 2008; Revised 12 February 2009; Accepted 3 March 2009
DOI: 10.1002/pro.111
Published online 16 March 2009 proteinscience.org

Abstract: Nature's high-performance polymer, spider silk, is composed of specific proteins, spidroins, which form solid fibers. So far, fibers made from recombinant spidroins have failed in replicating the extraordinary mechanical properties of the native material. A recombinant miniature spidroin consisting of four poly-Ala/Gly-rich tandem repeats and a nonrepetitive C-terminal domain (4RepCT) can be isolated in physiological buffers and undergoes self assembly into macrofibers. Herein, we have made a first attempt to improve the mechanical properties of 4RepCT fibers by selective introduction of AA → CC mutations and by letting the fibers form under physiologically relevant redox conditions. Introduction of AA → CC mutations in the first poly-Ala block in the miniature spidroin increases the stiffness and tensile strength without changes in ability to form fibers, or in fiber morphology. These improved mechanical properties correlate with degree of disulfide formation. AA → CC mutations in the forth poly-Ala block, however, lead to premature aggregation of the protein, possibly due to disulfide bonding with a conserved Cys in the C-terminal domain. Replacement of this Cys with a Ser, lowers thermal stability but does not interfere with dimerization, fiber morphology or tensile strength. These results show that mutagenesis of 4RepCT can reveal spidroin structure-activity relationships and generate recombinant fibers with improved mechanical properties.

Keywords: dragline silk; major ampullate spidroin; site-directed mutagenesis; disulfide bond

Introduction

Spider silk is nature's high-performance biopolymer with extraordinary mechanical properties. Its remarkable and unsurpassed toughness is due to a unique combination of high tensile strength and elasticity.[1] Spiders can make up to seven different silks using specialized glands. Dragline silk, which is used as a safety line or for radial orb web fibers, is one of the toughest of all fibers analyzed.[2] Dragline silk contains two proteins with similar amino acid sequences, referred to as major ampullate spidroin (MaSp) 1 and MaSp2.[3] MaSps are mainly composed of highly repetitive amino acid sequences, with recurrent poly-Ala blocks interrupted by Gly-rich regions. Spidroins also contain nonrepetitive N- and C-terminal domains of about 100–150 amino acids but with different sequences.[4] The C-terminal domain can form disulfide-mediated dimers and is important for fiber formation.[5–9] So far, fibers from recombinant spidroins, as well as fibers made from regenerated silk have failed in replicating the extraordinary mechanical properties of the spider's dragline. It has been suggested that the spider's

Abbreviations: 4RepCT, miniature spidroin with 4 poly-Ala/Gly-rich repeats and nonrepetitive C-terminal domain; CD, circular dichroism; MaSp, major ampullate spidroin; SEC, size exclusion chromatography; SEM, scanning electron microscopy.

S.G., J.J., and M.H. have shares in Spiber Technologies AB, a company that aims to commercialize recombinant spider silk.

Grant sponsor: European Commission; Grant number: G5RD-CT-2002-00738; Grant sponsor: The Swedish Research Council; Grant number: 10371; Grant sponsor: FORMAS; Grant number: 221-2006-2336.

*Correspondence to: M. Hedhammar, Department of Anatomy, Physiology and Biochemistry, Swedish University of Agricultural Sciences, the Biomedical Centre, Box 575, 751 23 Uppsala, Sweden. E-mail: my.hedhammar@afb.slu.se

intricate spinning procedure and the large sizes of the native spidroins are of key importance for obtaining a very strong biopolymer, but crucial factors contributing to the silk characteristics still remain elusive.[10–12]

The impressive mechanical properties of spider dragline silk combined with its biocompatibility[13–15] make this material an interesting target for use as a biomaterial, with potential applications in tissue engineering.[16] For example, the use of spidroin fibers as scaffolds for generation of bone, ligaments, and nervous tissue replacements has been envisioned.[14,17–20] However, such attempts have been hampered by the inability to obtain sufficient quantities of native spider silk, or fibers from recombinant spidroins. Full length MaSp polypeptides are large, containing 3–4000 residues,[21] and no attempts to produce full length spidroins recombinantly have been published so far. Several ways to produce recombinant spidroin fragments or simplified sequences inspired by the MaSp poly-Ala/Gly-rich pattern have been established[22] but subsequent formation of fibers has proved more challenging. Some of these systems yield high amounts of protein, but the repetitive and hydrophobic character of the spidroins makes them prone to aggregate in aqueous solutions, why the use of denaturing agents or salts for resolubilization often is required.

Our group recently introduced a new way to produce an *Euprosthenops australis* MaSp1 fragment that allows isolation using aqueous buffers and spontaneous formation of macroscopic-sized fibers.[8,9] This was possible by the use of a comparatively short MaSp1 fragment, containing only four poly-Ala/Gly-rich regions and the nonrepetitive C-terminal domain, 4RepCT, and a cleavable fusion partner that prevents aggregation during protein production and isolation. The amenability of this system for site-directed mutagenesis raises interesting possibilities such as rational design of customized fibers, and also gives the opportunity to test the importance of specific spidroin sequence features for fiber formation. Herein, we investigate whether the mechanical properties of the recombinant MaSp1 fibers can be improved by introduction of intermolecular disulfide bridges between poly-Ala blocks, which lack Cys in the native fibers. Moreover, the importance of the native disulfide-mediated dimerization of the nonrepetitive C-terminal domain for fiber formation is investigated.

Results

Three mutants based on 4RepCT were generated; CC1, CC2, and S (see Fig. 1). Two adjacent Ala were altered to Cys in the middle of either the first or fourth poly-Ala block. As the poly-Ala blocks are thought to form β-sheets in the fibers, adjacent Cys side-chains will point in opposite directions, which was assumed to maximize the chances of forming intermolecular disulfides. In S, the conserved Cys in the nonrepetitive C-terminal domain was changed to Ser, to investigate the importance of this Cys for dimerization and fiber formation.

Effects of mutations on expression, secondary, and quaternary structure and thermal stability

The miniature spidroins were expressed as fusions with a HisTrxHis tag, which was removed after proteolysis by subsequent IMAC purification. All purification steps were done under nondenaturing conditions, which yielded soluble, highly pure (>95% judged by SDS-PAGE) 4RepCT, CC1, and S [Fig. 1(B)]. On SDS-PAGE under nonreducing conditions S migrates as a monomer while 4RepCT and CC1 migrates as dimers [Fig. 1(B)], confirming the disulfide mediated dimerization through the Cys in the C-terminal domain.

In contrast to 4RepCT and the CC1 and S mutants, the CC2 spidroin was not recovered in the soluble fraction after cell lysis, although produced by the cells, as shown by SDS-PAGE of pellets dissolved in 8*M* urea [Fig. 1(B)]. 4RepCT and CC1 could likewise be found in pellets after cell lysis, but to a much lower extent than for CC2. Attempts to obtain soluble CC2 by adding reducing agents to the cell lysis- and purification buffers were not successful.

The far-UV CD spectra of 4RepCT, CC1, and S are very similar, indicating that their secondary structure contents do not differ significantly [Fig. 2(A)]. The melting curve for S shows that this mutant, lacking the disulfide bridge between C-terminal domains, is slightly less temperature stable than 4RepCT [Fig 2(B)]. Reduced 4RepCT is equally temperature stable as the nonreduced protein, and the CD changes are not reversible by cooling (not shown). In line with this, most of the protein has gone out of solution after heating and small aggregates appear in the cuvette. Thus, the thermal melting curve of 4RepCT captures both unfolding and conversion to β-sheet aggregates. The melting curve of CC1 is shifted to the right compared to 4RepCT, both under nonreducing and reducing conditions. CC1 does not form disulphide-dependent oligomers in solution [Fig. 1(B)], which suggests that the shift of the curve is more likely caused by a reduced tendency for conversion into β-sheet aggregates, rather than an increased stability due to disulphide bridges.

Upon size exclusion chromatography (SEC), S, CC1, and 4RepCT elutes at the same position, which corresponds to a molecular mass of ~46 kDa, indicating that all three proteins are dimers (data not shown).

Fiber formation and appearance

Macroscopic fibers were formed spontaneously and with similar kinetics for 4RepCT, CC1, and S, independent of the conditions used (see Table I). For all three variants, the major part of the protein resulted in well-defined fibers, with only a minor fraction (<5%) trapped in aggregates, and no detectable

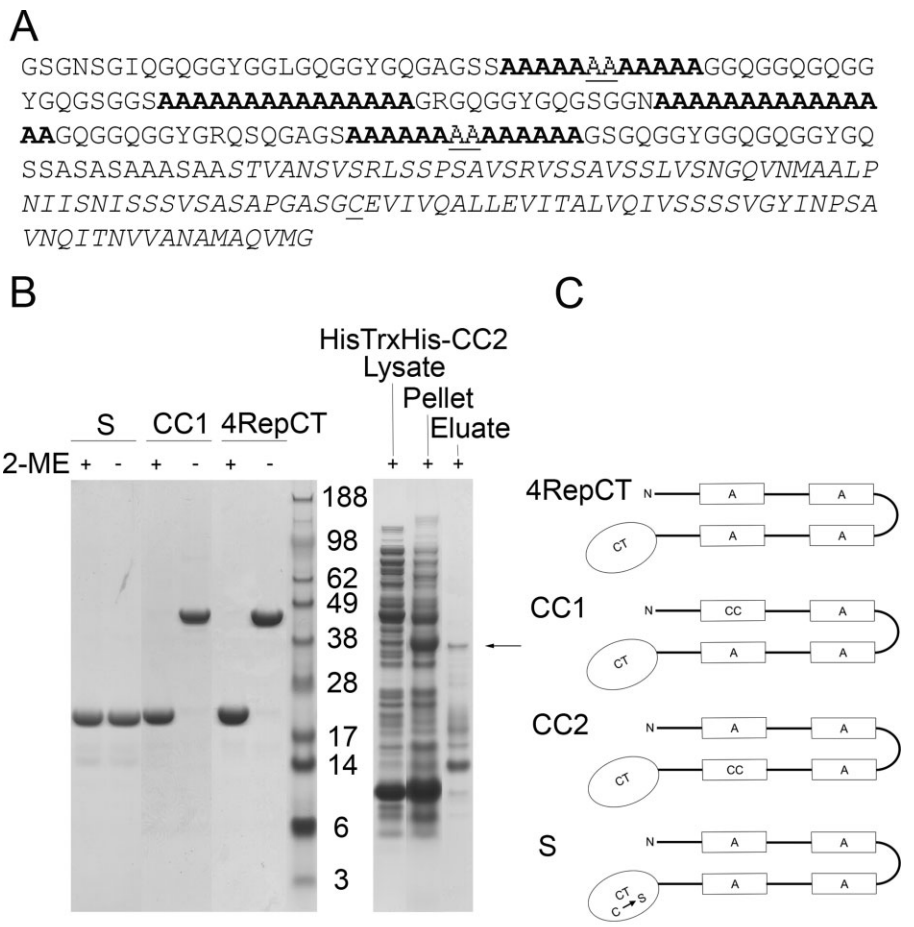

Figure 1. Properties of the proteins analyzed. (A) Primary structure of 4RepCT. The poly-Ala blocks are in bold and the C-terminal domain is in italics. Mutated residues in CC1, CC2, or S are underlined. (B) Left: SDS-PAGE of purified S, CC1, and 4RepCT, under reducing and nonreducing conditions ± mercaptoethanol (2-ME). Migration of low-molecular mass markers (kDa) is shown in the middle. The gel on the right side depicts reduced samples of HisTrxHis-CC2 cell lysate, urea dissolved pellet and isolated protein. Migration of HisTrxHis-CC2 is marked by an arrow. (C) Schematic description of 4RepCT, CC1, CC2, and S. White boxes labeled A represent poly-Ala stretches, and black lines represent Gly-rich regions. CC corresponds to the AA → CC mutations, and the C (S mutation in the C-terminal domain is indicated.

protein in the final soluble fraction. The macroscopic appearances of 4RepCT, CC1, and S fibers in a wet state were similar (see Fig. 3). Air-drying of the fibers while fixed in a straightened state resulted in homogenous fibers and no differences in morphology could be detected under a light microscope or by scanning electron microscopy (SEM) (see Fig 3). The different conditions used for promoting disulfide linkage during fiber formation did not affect the fiber morphology (Fig. 3 and data not shown).

Determination of the diameter was done nondestructively for each fiber using light microscopy. The diameter varied from 40 and 90 μm between different fibers. Birefringence of fibers makes diameters measured by light microscopy overestimated.[23] However, this will not affect the conclusions from this study, as they are based on comparisons between different fibers measured in the same manner.

CD spectra of suspensions of the different fibers all showed a minimum at 220 nm and a maximum at 193 nm (data not shown), as shown before for 4RepCT fibers,[8] indicating a substantial fraction of β-sheet structure.

Effects of intermolecular disulfides on mechanical properties of the fibers

Fibers from CC1 (and 4RepCT as a control) were made under different conditions to promote disulfide formation and formed fibers were treated with DMSO or O_2 with the same purpose. See Table I for a survey of conditions used.

During tensile testing most fibers, irrespective of minispidroin and treatment, broke at the grip point. This may be caused by structural defects introduced by fixation or as a consequence of that the fibers are difficult to align perfectly with the direction of pulling. For this reason we studied a large number of different fibers to be able to analyze the results statistically. However, breakage at the grip point may result in an underestimation of the maximum stress and maximum

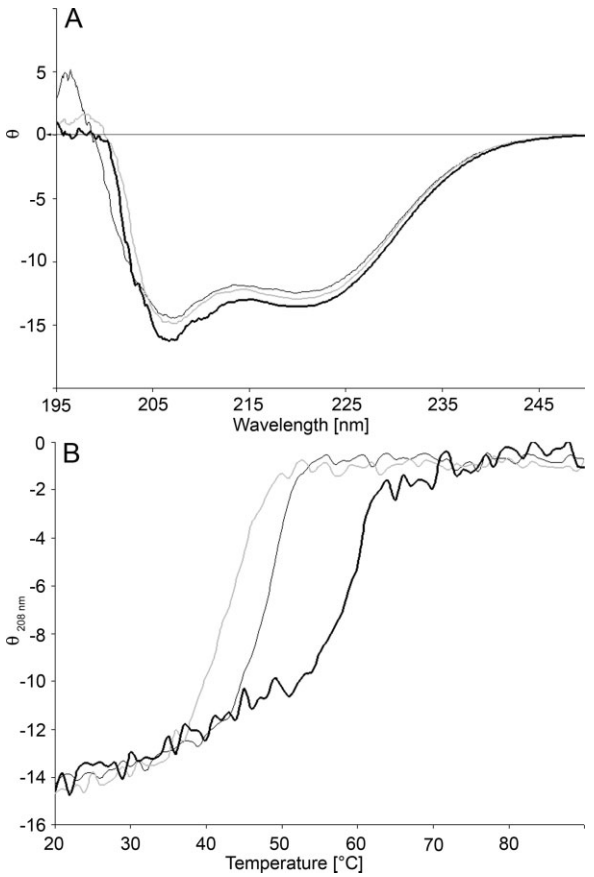

Figure 2. Secondary structure and temperature stability of 4RepCT, CC1 and S. (A) CD spectra of 4RepCT (dark grey), S (light grey) and CC1 (black) at 20°C. (B) Thermal unfolding of 4RepCT (dark grey), S (light grey), and CC1 (black). The residual molar ellipticity at 208 nm (θ) is expressed in kdeg × cm^2 × $dmol^{-1}$.

strain. These values are therefore used mainly to compare different groups, and comparisons with literature data should be made with caution.

The initial modulus was higher, with statistical significance, for all fibers made from CC1 compared with those made from 4RepCT (Fig. 4, Tables II and III). Further analysis of a large number of fibers from two different batches of minispidroins analyzed at two different occasions confirmed this conclusion ($n = 10$ and $n = 25$ for 4RepCT and $n = 30$ and $n = 51$ for CC1. P values 0.0037 and < 0.0001, respectively). Also the maximum stress tolerated before breakage was higher for all fibers made from CC1, except for CC1 fibers treated with 10% of DMSO (Fig. 4, Tables II and III). Different buffer conditions (Table I) were used to find optimal redox-conditions. The CC1 fibers made in the presence of 3 m*M* reduced glutathione (GSH) 0.3 m*M* oxidized glutathione (GSSG) appeared to have higher initial modulus than the other CC1fibers, but the differences did not reach statistical significance (Fig. 4, Tables II and III). The maximum strain tolerated before breakage did not show any clear trend between 4RepCT and CC1 fibers, while S fibers tolerated less strain than 4RepCT fibers (Fig. 4, Tables II and III). The initial modulus and maximum stress, however, did not differ significantly between 4RepCT and S fibers (Fig. 4, Tables II and III).

Irrespective of redox conditions used, appearances upon nonreducing SDS-PAGE of CC1 before onset of fiber formation were very similar to that of 4RepCT and showed no protein larger than dimer (in which the subunits are held together with a disulfide between two C-terminal domains). However, the presence of GSH promotes reduction of the disulfide between the C-terminal domains [Fig. 5(A)]. To evaluate to what extent intermolecular disulfide linkages had formed during or after fiber formation, fibers were dissolved in formic acid and analyzed by SDS-PAGE under reducing and nonreducing conditions. CC1 fibers showed bands corresponding to tetramers, which disappeared after reduction [Fig. 5(B)]. This indicates that the Cys introduced in the first Ala block mediate intermolecular disulfide formation. Moreover, the extent of disulfide formation can be modulated by varying the conditions under which fibers are formed. CC1 fibers self-assembled in the presence of GSH/GSSG also showed bands corresponding to penta- and

Table I. *Conditions and Miniature Spidroins Used for Fiber Formation and Post-Treatment*

			Fiber type		
	Redox treatment	pH	CC1	4RepCT	S
	No treatment	8.0	X	X	X
		9.5	X	X	
Fibers formed in GSH/GSSG	3 m*M*/0.3 m*M*	8.0	X	X	
		9.5	X		
	0.3 m*M*/3 m*M*	8.0	X	X	
		9.5	X		
	1.65 m*M*/1.65 m*M*	8.0	X		
	0/5 m*M*	8.0	X		
Fibers incubated in	10% DMSO	8.0	X		
	Oxygen	8.0	X		

X denotes fibers tested for tensile strength and analyzed by SDS-PAGE.

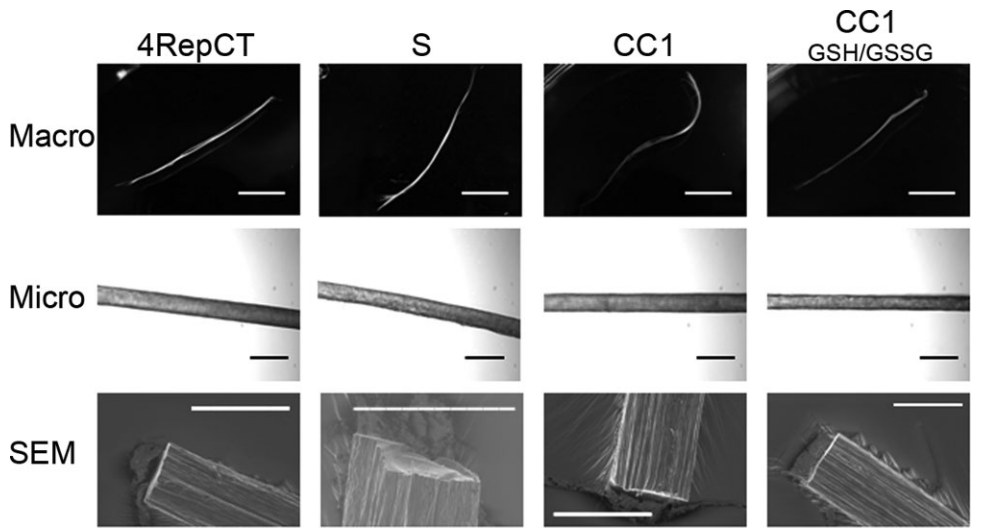

Figure 3. Fiber morphology. Macroscopic, light microscopic and SEM pictures of fibers made from 4RepCT, S, CC1, and CC1 fibers formed in 3 m*M* GSH/0.3 m*M* GSSG. The macroscopic pictures show fibers in buffer before drying, the light microscopic pictures are of dried fibers before tensile testing and the SEM images depict fibers after tensile testing. The scale bar is 1 cm in the macroscopic pictures and 100 μm in light microscopic and SEM images.

hexamers [Fig. 5(B)]. However, only a rather minor fraction of molecules are linked via disulfides between Cys in Ala blocks, because dimeric CC1 (in which the dimers are formed *via* the disulfide between the C-terminal domains) dominates in all fibers (see Fig. 5).

Discussion

The extreme mechanical properties of spider silk have since long attracted the attention of researchers aiming to design durable materials for a number of purposes.[16] MaSp genes sequenced so far are large,[21] which indicates that a large number of repeat units improve mechanical properties. Large fibroin genes is also a feature independently selected for in insects[16,21]

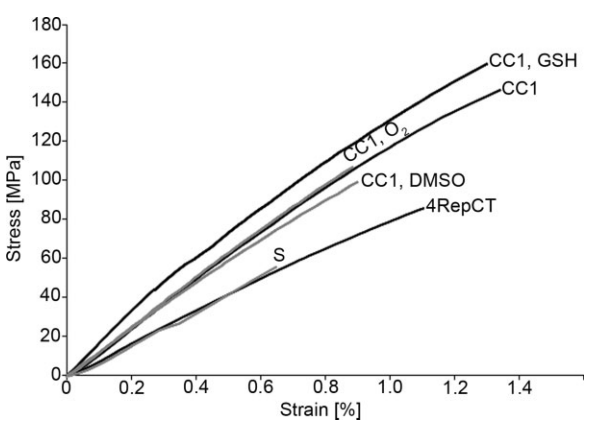

Figure 4. Mechanical properties of fibers. Stress versus strain for median fibers within each group. For fiber groups with even number of fibers tested, the one with the highest initial modulus of the two middle fibers is displayed. CC1, GSH stands for CC1 made in 3 m*M* GSH/0.3 m*M* GSSG; CC1, O_2 stands for CC1 treated with O_2; and CC1, DMSO stands for CC1 treated with 10% DMSO.

which further implies that large silk proteins are beneficial for producing strong silks. In line with the supposition that spidroin length correlates with strength of fibers, many attempts to produce recombinant silks have aimed at maximizing length of spidroins used. This ambition, however, is likely to give also decreased yields and lowered solubility, which has resulted in frequent use of denaturing agents and organic solvents for solubilization to allow artificial spinning from a concentrated spidroin dope.[22] Several strategies to convert the spidroin dope into solid fibers have been tried, including variants of wet spinning[11,24–29] and electro spinning.[28,30] Most artificial spinning strategies require post-treatment in dehydrating solvent and further postspinning procedures that increase β-sheet content and structural orientation in the fibers, before demanding handling procedures such as mechanical testing are practically possible. So far, recombinantly produced spidroin analogues that have been denatured and artificially spun have given rise to fibers that are much weaker than the native spider silk, both in terms of stress and initial modulus, no matter of the length of the protein.[11,24–29] Not even artificial spinning of regenerated natural spider silk, likely containing full-length spidroins in a denatured form, has delivered fibers that match native spider silk.[10,12] The mechanical properties of silk reeled from spiders vary with factors such as speed and environmental conditions during spinning.[31] This implies that both the protein size and the spinning conditions affect the properties of the resultant fibers. Moreover, the structure of the soluble spidroin might be important for an optimal conversion into a solid fiber.[8,9] The relative importance of protein sequence, length, and structure compared to the spinning conditions remain to be delineated.

Table II. *Mechanical Properties of 4RepCT, CC1 and S fibers, Made Under Different Conditions*

Protein	Treatment	*n*	Mean maximum stress (MPa) ± SD	Mean maximum strain (%) ± SD	Mean initial modulus (GPa) ± SD
4RepCT	—	16	80 ± 20	1.0 ± 0.1	9 ± 2
CC1	—	9	110 ± 30	1.2 ± 0.3	12 ± 4
CC1	DMSO[a]	8	90 ± 20	0.9 ± 0.1	12 ± 3
CC1	O_2[b]	10	100 ± 30	0.9 ± 0.1	13 ± 3
CC1	GSH/GSSG[c]	16	110 ± 30	1.0 ± 0.3	14 ± 4
S	—	8	80 ± 30	0.9 ± 0.2	10 ± 4

[a] Fibers treated over night in 20 m*M* Tris-HCl, pH 8 containing 10% DMSO.
[b] Fibers treated 3 h with gentle bubbling of O_2.
[c] Fibers formed in 20 mM Tris-HCl, pH 8, with 3 mM GSH/0.3 mM GSSG

If medical applications of the synthetic spider silk are the main objective, it needs to be biocompatible, which further complicates the endeavor of finding suitable production methods that do not include noxious solvents. Thus, production of long spidroins that do not aggregate before fiber formation have been attempted. Genetic introduction of Met residues in a recombinant consensus repeat of dragline silk from *N. clavipes* allowed control of assembly via oxidation and reduction; oxidation prevented assembly, whereas reduction allowed assembly as for the nonmodified protein.[32,33] In a similar manner, a genetically introduced kinase recognition motif allowed control of assembly via enzymatic phosphorylation/dephosphorylation.[34] However, no fibers were formed from these constructs.

In an attempt to survey spontaneous fiber formation we recently investigated a miniature spidroin, 4RepCT, produced recombinantly in soluble form under nondenaturing conditions, and then induced to assemble into macroscopic fibers.[8] The mechanical strength of 4RepCT fibers[8] compares favorably to artificial silk made from larger but denatured spidroins,[27–29] but it is below that of native dragline silks. To improve the mechanical properties of fibers made of the comparatively small 4RepCT, we envisioned that covalent multimerization could be employed. Herein it is shown that the initial modulus of 4RepCT fibers can be improved by introduction of covalent linkages between poly-Ala blocks. The present study is the first where the mechanical properties of recombinant spider silk has been increased by genetic engineering.

The fibers of 4RepCT are self assembled in an aqueous environment without the usage of any spinning apparatus and rely thus on the organizational ability of the protein. CD spectra and X-ray diffraction[8] of the 4RepCT fibers show a substantial fraction of β-sheet structure although the orientation is lower than in the native fibers (L. Serpell, personal communication). The mechanical properties can be improved by postdrawing of the wet fibers,[8] which probably increases the molecular orientation. The alignment through postdrawing and the presence of water have a great impact on the strength of artificial silks.[10,35] To avoid multiple handlings steps when comparing 4RepCT with genetic variants thereof, the mechanical analysis is herein done directly on self assembled and dried fibers. This, in combination with biochemical analysis of disulfide formation, is used to correlate mechanical properties with cross-linking of the protein chains. As the mechanical properties of spider silk are affected by conditions, including climate at testing[2,36] only fibers tested at the same occasion are compared.

Natural spider silk has been identified as a semicrystalline material made of amorphous, flexible chains reinforced by strong and stiff crystals.[37] In the fibers, the Gly-rich regions of the spidroins likely form amorphous regions that are important for elasticity while the poly-Ala blocks are thought to form

Table III. *Statistical Analysis of Mechanical Properties Using Students Unpaired-t Test*

	Properties compared and *P* values		
Compared groups	Mean maximum stress	Mean maximum strain	Mean initial modulus
4RepCT/CC1, GSH/GSSG	0.001	0.22	<0.0001
4RepCT/CC1	0.001	0.12	0.02
4RepCT/CC1, DMSO	0.28	0.01	0.01
4RepCT/CC1, O_2	0.02	0.01	0.0001
4RepCT/S	0.94	0.01	0.24
CC1/CC1, GSH/GSSG	0.91	0.05	0.13
CC1/CC1, DMSO	0.06	0.02	0.89
CC1/CC1, O_2	0.52	0.01	0.38

See Table II for exact treatment procedures.

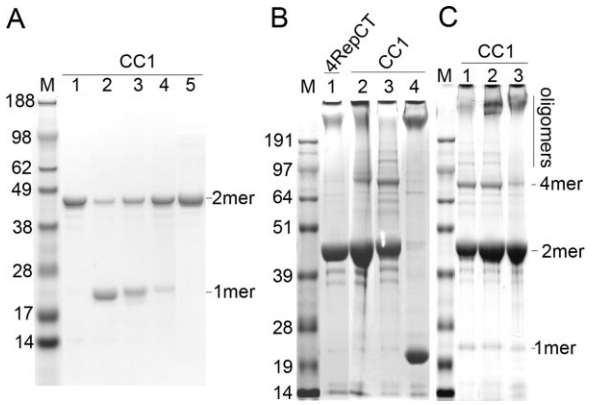

Figure 5. Intermolecular disulfides in soluble minispidroins and fibers. (A) SDS-PAGE of CC1 in the presence of different GSH/GSSG concentrations before fiber formation. Lane 1, no GSH/GSSG; lane 2, 3 m*M* GSH/0.3 m*M* GSSG; lane 3, 1.65 m*M* GSH/1.65 m*M* GSSG; lane 4, 0.3 m*M* GSH/3 m*M* GSSG; lane 5, 5 m*M* GSSG. (B) Fibers of 4RepCT and CC1 formed under different conditions dissolved in formic acid as described in the "Materials and Methods" section, and analyzed for intermolecular covalent linkages by SDS-PAGE. Lane 1, 4RepCT formed in 3 m*M* GSH/0.3 m*M* GSSG; Lane 2 CC1 formed with no GSH/GSSG; lane 3, CC1 formed in 3 m*M* GSH/0.3 m*M* GSSG; lane 4, same as in lane 3 but analyzed under reducing conditions. (C) Dissolved fibers of CC1 formed in the presence of different GSH/GSSG concentrations. Lane 1, 1.65 m*M* GSH/1.65 m*M* GSSG; lane 2, 0.3 m*M* GSH/3 m*M* GSSG; lane 3, 5 m*M* GSSG. M lanes show molecular mass markers (kDa).

intermolecular β-sheets that mediate the tensile strength.[37] A calculated stress strain curve based on this model gives a value of the initial modulus of 10 GPa,[37] which is in good agreement with experimental observations of native spider silk.[36] According to this model hydrogen bonds start to break at a tensile strength of 100 MPa and ~2% elongation leading to the formation of a yielding point.[37,38] These features of a stress strain curve have later been experimentally shown to be typical for silk.[39–42] Tensile testing of self assembled, dried 4RepCT fibers (see Fig. 4) shows a linear stress-strain relationship and no clear yielding point, in good agreement with predictions for a crystalline and brittle material. The initial modulus is comparable to that of native spider silk but the point where 4RepCT breaks corresponds roughly to the yield point of its native counterpart.[23,40–47] The lack of strain-hardening might be due to the comparatively short polypeptide chain of 4RepCT, which probably limits entanglements.[48,49]

The stress-strain curve of CC1 resembles that of 4RepCT, with the main difference being a higher initial modulus and a higher breaking stress (Fig. 4, Table II). The CC1 mutations do not alter the ratio between the primary structure elements thought to contribute to crystallinity (poly-Ala blocks) and elasticity (Gly-rich blocks) but allow intermolecular disulfides to form between poly-Ala blocks, see further below. Apparently this results in increased initial modulus without change in extensibility. This implies that the stiffness of the fibers is mainly due to the interconnecting forces between β-strands.

In CC1 and CC2, the two central Ala in the first and fourth poly-Ala block, respectively, were substituted for Cys (see Fig. 1). The fact that CC2 could not be recovered in soluble form implies that the positioning of the Cys is of importance, and that future attempts to modulate fiber mechanical strength by introduction of Cys need to cover a large set of mutants. The drastically different consequences of introduction of Cys in the fourth (i.e., most C-terminal) compared to in the first (i.e., most N-terminal) poly-Ala block might be due to disulfide formation with the naturally occurring Cys in the C-terminal domain, which is highly conserved among major ampullate spidroins.[50] Alternatively, the Cys in the fourth poly-Ala block gives increased availability for intermolecular disulfide bridges that collapses the soluble structure. The fact that fibers could be formed from both mutant spidroins that could be produced in soluble form, CC1 and S, suggests that the fiber formation is quite robust. This makes it likely that further genetically engineered variants can be successfully expressed and used to form fibers.

It has been suggested that the C-terminal domain directs fiber formation[9] and contributes to the mechanical properties of the fibers by mediating covalent linkage.[51] In the S mutant the Cys in the C-terminal domain was changed to Ser (see Fig. 1). Fibers made from S had occasionally a more fimbriated appearance compared to 4RepCT and CC1 fibers. However, the maximum stress tolerated and the initial modulus of S fibers are not significantly different from those of 4RepCT fibers, while they tolerate less strain before breakage (Fig. 4, Tables II and III). These results, together with the data for CC1 fibers, suggest that the stiffness of 4RepCT based fibers is largely independent on covalent interactions between nonrepetitive C-terminal domains, but relies mainly on intermolecular interactions between poly-Ala blocks.

To covalently multimerize CC1, Cys in the poly-Ala block must form intermolecular disulfide bridges. This likely requires a precise molecular alignment and oxidizing conditions. As fiber formation involves a structural change it is important that formation of disulfides that hinders this conversion is avoided. GSH/GSSG is often used to allow disulfide shuffling during refolding and renaturation procedures when proteins are purified from inclusion bodies dissolved in urea or other denaturing agents.[52,53] Analysis of the soluble CC1 in the presence of different GSH/GSSG ratios shows that the redox conditions used allow reduction of disulfides giving rise to monomeric CC1 [Fig. 5(A)]. No higher order oligomers than dimers can be seen in the soluble fraction. In contrast,

analysis of the oligomerisation status of dissolved CC1 fibers shows tetramers, and even higher oligomers, from fibers formed under redox conditions. In parallel, it appears that fibers made from CC1 in the presence of GSH/GSSG results in stronger fibers compared to when they are allowed to form without redox agents (Fig. 4, Tables II and III). In an attempt to favor high-oligomeric CC1 fibers, different redox conditions were used (Table I) to find optimal conditions. However, differences, if existent, were too small to be verified by tensile testing and SDS-PAGE analysis. However, it is clear that CC1 allows oligomerisation (see Fig. 5) and gives mechanically stronger fibers, since all CC1 fibers, irrespective of treatment, were significantly improved compared to the 4RepCT fibers (Fig. 4, Tables II and III).

The self-assembled fibers analyzed herein are much thicker (= 40–90 μm) than natural dragline silk, that is usually only a few microns thick.[23,35,54] However, fibers of 4RepCT and mutants thereof are composed of smaller subfiber filaments down to a diameter of ~200 nm.[8] The tensile strength of a bundle is generally less than that of the individual components. Therefore, possible differences in mechanical strength between CC1 filaments formed under different redox conditions may be masked in the current experimental setup. This possibility could be analyzed using smaller scale indentation measurements, for example by atomic force microscopy.

To avoid disulfide formation before and during fiber formation, oxidizing treatments can be applied to formed fibers. DMSO is able to oxidize free thiols to disulfides. However, post-treatments of CC1 fibers with DMSO did not improve the mechanical properties of the CC1 fibers compared to the other methods employed. Possibly, post-treatment of fibers is comparatively inefficient, if the polypeptide chains are locked in conformations where Cys can not form disulfides, but other reasons for the differences can not be excluded. Also the fibers that were bubbled in oxygen did not show improved mechanical properties, further suggesting that post-treatments are less efficient.

Disulfide bonds; one of natures way to covalently link polypeptide chain(s) and thereby confer stability, is used frequently in widely different proteins, for example, immunoglobulins,[55] antimicrobial peptides[56] and keratin.[57] Most silks are covalently stabilized by disulfide bonds, although not all through a Cys in the C-terminal domain, as in MaSps. Egg-case protein-1 and 2 in the silk from the tubuliform gland of the cobweb weaver *Latrodectrus hesperus* contain a large number of Cys in the N-terminal region, believed to mediate higher-aggregate complexes.[58] It is noted that after prolonged treatment of solubilized egg case material with reducing agents there is an increase in monomers.[59] The heavy and the light chain of the fibroin comprising the monofilament of the silkworm, *Bombyx mori*, are interconnected through a disulfide bridge with implications for structure and mechanical properties of the silk. Disulfide dependent cross-linking of proteins is also speculated to be a crucial factor in the structure and polymerization of silk produced by the larvae of *Chironomus tentans*, which is spun into insoluble threads used to construct underwater feeding and pupation tubes.[60]

Other intermolecular connectors have been speculated to be of importance for the strength of spider silk. Some Arthropods rely on cross-linking of molecules in resilient structural materials through Tyr-Tyr connections, possibly enhancing the mechanical properties of the polymers.[61–63] Together with indication of peroxidase activity in the major ampullate gland of the *Nephila edulis* spider,[2] it was suggested that spidroins can be interconnected through covalent Tyr-Tyr formation, but experimental evidence could not be documented.[2] However, Tyr-Tyr connections might be an alternative way of improving mechanical properties of recombinant spider silk through genetic engineering and optimized conditions during fiber formation.

In conclusion, a 4RepCT miniature spidroin was used to address questions related to the structural basis for fiber formation and strength. It was found that artificial silks made from recombinant spidroins can be tailored to improve their mechanical properties without using potentially noxious cross-linking agents, and that the conserved Cys in the C-terminal domain is not necessary for dimer formation or fiber self-assembly.

Materials and Methods

Construction of mutants

pET32TrxHisS[8] containing a cDNA fragment encoding four poly-Ala and Gly-rich blocks followed by the C-terminal domain of MaSp1 from *E. australis,* denoted 4RepCT, was used as template for generation of three mutants, named CC1, CC2, and S (see Fig. 1 for a description of the structures of the mutants and 4RepCT). For construction of these mutants, QuickChange (II Site-Directed Mutagenesis Kit (Stratagene) and the following primers were used: CC1-sense (5′-GTT CTG CAG CCG CTG CCG CCT GCT GCG CAG CCG CCG CAG CAG GTG G-3′), CC1-antisense (5′-CCA CCT GCT GCG GCG GCT GCG CAG CAG GCG GCA GCG GCT GCA GAA C-3′), CC2-sense (5′-CCG CTG CTG CTG CTG CTG CTT GTT GTG CCG CTG CTG CTG CTG CAG G-3′), CC2-antisense (5′-CCT GCA GCA GCA GCA GCG GCA CAA CAA GCA GCA GCA GCA GCA GCG G-3′), S-sense (5′-GCT CCT GGT GCT TCT GGA TCT GAG GTC ATA GTG CAA GCT C-3′), and S-antisense (5′-GAG CTT GCA CTA TGA CCT CAG ATC CAG AAG CAC CAG GAG C-3′). The resulting PCR products were *Dpn* I treated and used to transform XL1-Blue Supercompetent Cells (Stratagene) for nick-repair and subsequent amplification. The constructs were checked for correct sequences and then restricted

with *Bam*HI and *Hind*III for subsequent ligation into the pHisTrxHis vector,[9] encoding a His_6 tag, thioredoxin, another His_6 tag and finally a thrombin cleavage site. The resulting constructs were denoted pHisTrxHisCC1, pHisTrxHisCC2 and pHisTrxHisS, respectively.

Expression and isolation of 4RepCT and mutants thereof

The three mutant constructs and pHisTrxHis4RepCT[9] were used to transform *E. coli* BL21 (DE3) cells (Merck Biosciences). The cells were grown to an OD_{600} of 0.8–1.2 at 30°C in Luria-Bertani medium containing kanamycin, and then induced with isopropyl β-D-thiogalactopyranoside, and further incubated for up to 2.5 h at 20°C. Thereafter, cells were harvested and resuspended in 20 m*M* Tris-HCl, pH 8.0, supplemented with lysozyme and DNase I. After complete lysis, the 15,000*g* supernatants were loaded onto a column packed with Ni-NTA Sepharose (GE Healthcare, Uppsala, Sweden). The column was washed extensively before bound proteins were eluted with 300 m*M* imidazole in 20 m*M* Tris-HCl, pH 8.0. Fractions containing the target proteins were pooled and dialyzed against 20 m*M* Tris-HCl, pH 8.0.

Purification of CC2 was performed as described earlier, and also in the presence of 2-mercaptoethanol (2-ME) (Sigma). 2-ME (0.5 m*M*) was added to the lysis buffer, and after 1 h, 2-ME was added to a concentration of 10 m*M*. The lysis reaction was continued for 30 min and thereafter 15,000*g* supernatants were loaded onto a Ni-NTA Sepharose (GE Healthcare, Uppsala, Sweden) column equilibrated with 20 m*M* Tris-HCl, pH 8.0, containing 10 m*M* 2-ME. Washing, elution and dialysis buffers were supplemented with 10 m*M* 2-ME.

Target proteins were released from the HisTrxHis tag by proteolytic cleavage using a thrombin:fusion protein ratio of 1:1000 (w/w) at 20°C for up to 1.5 h. Prolonged proteolysis results in unspecific cleavage, probably at an RG-site in the spidroins, and further proteolysis was therefore blocked by addition of Pefabloc (Fluka, Germany) to 1 m*M*. The released HisTrxHis tag was removed by passage over a Ni-NTA Sepharose column and the target protein was eluted with 20–30 m*M* imidazole in 20 m*M* Tris-HCl, pH 8.0. Proteins were analyzed by SDS-PAGE and staining with Coomassie Brilliant Blue R-250. Purified proteins were concentrated by ultra-filtration over a 3 kDa cut-off cellulose filter (Millipore). Protein contents were determined from the OD_{280} and calculated molar extinction coefficients.

Circular dichroism spectroscopy and size exclusion chromatography

Circular dichroism (CD) spectra from 250 to 190 nm were recorded in a 0.1-cm path length quartz cuvette using a J-810 spectropolarimeter (Jasco, Tokyo, Japan). The scan speed was 50 nm/min, response time 2 s, acquisition interval 0.1 nm, and bandwidth 1 nm. Typically, protein concentrations of 20–30 μM in 20 mM Tris, pH 8.0, were used. For reduction, dithiothreitol was added to 2 m*M* and the samples incubated for at least 45 min at 20°C. Temperature scans from 20 to 90°C, 0.5°C increase/min, were performed using cuvettes equipped with a Teflon lid. After measurement at 90°C, the samples were cooled to 20°C, equilibrated for 20 min and scanned again. For thermal unfolding curves, the residual molar ellipticities at 208 nm were used, since the change in signal was found to be most pronounced at this wavelength. For CD measurements of fibers, they were cut into small pieces and suspended by vigorous vortexing in 2% SDS buffer.

SEC of soluble 4RepCT, CC1, and S was performed using a Sephacryl S-100 HR (GE Healthcare) column, with 1.0-cm inner diameter and 37-cm bed height, equilibrated with 20 m*M* Tris, pH 8.0, and an ÄKTA basic system (GE Healthcare) at a flow rate of 0.5 mL/min.

Fiber production and promotion of disulfide formation

Fibers were made essentially as previously described.[8] 4RepCT, CC1, or S proteins in 20 m*M* Tris-HCl, pH 8.0, were incubated in glass tubes at room temperature until no soluble protein could be detected in the supernatant (>48 h), implying that essentially all protein had polymerized into fibers.

To promote formation of intermolecular disulfide bridges, fibers were either made under different redox conditions or treated in different ways after fiber formation was completed. For Cys oxidation during fiber formation, reduced (GSH) and oxidized (GSSG) glutathione (Saveen & Werner AB, Sweden) in 20 m*M* Tris-HCl, pH 8.0, or 9.5 were used in the following ratios: (i) 3 m*M* GSH/0.3 m*M* GSSG; (ii) 1.65 m*M* GSH/1.65 m*M* GSSG; (iii) 0.3 m*M* GSH/3 m*M* GSSG; and (iv) 5 m*M* GSSG (see Table I).

For post-treatment of fibers, dimethyl sulfoxide (DMSO) or O_2 was used. For DMSO treatment, fibers were agitated by rocking in 20 m*M* Tris-HCl, pH 8.0, containing 10% (v/v) DMSO at 20°C over night. For O_2 treatment, fibers in 40 mL of 20 m*M* Tris-HCl, pH 8.0 were gently bubbled with O_2 (medical oxygen class 2, Air Liquide, Sweden) for 3 h at 20°C. The buffer was saturated by vigorous bubbling for 30 min prior to adding the fibers.

After the different treatments, the fibers were gently stretched until straight, as judged by visual inspection, and air-dried for ~20 min, when no further visible change of the fiber could be detected. The dried fibers were stored in capped plastic tubes at 22°C until further analysis.

Determination of fiber diameter and scanning electron microscopy

Dried fibers were photographed using a Leica DMLB light microscope at 20× magnification. The diameter was determined at 3–5 positions along each fiber using a length reference and the imageJ software, whereof the lowest value was used.

Representative fibers (before and after drying and tensile testing) were applied on SEM stubs where they were air-dried and vacuum coated with gold and palladium. The samples were photographed with a LEO 1550 FEG microscope (Carl Zeiss, Oberkochen, Germany) using an acceleration voltage of 5 kV.

Tensile strength measurements

Stress versus strain (% length extension) of dried fibers was measured under ambient conditions (~22°C, 30–40% relative humidity) with a DMA Q800 V7.4 (TA instruments) using a ramp force of 0.2 N/min. The fiber ends were glued with a small amount of cyanoacrylate (Loctite® Super Attak®) between thin sheets of cardboard paper and mounted in the clamps. The fibers were fixed with the same force each time. Fibers with macroscopic defects or that were obviously maltreated during mechanical testing were excluded (<10% of all fibers). A circular initial cross section of the fibers was used for the calculation of stress. The data was analyzed with the TA Universal Analysis software (TA instruments).

Assessment of intermolecular disulfide formation in fibers

Dried fibers, ~3 cm in length, were dissolved in neat formic acid supplemented with SDS. The solvent was evaporated and pellets were suspended in 60 μL gel loading buffer containing SDS, resulting in a final SDS concentration of 6%. For reduced samples the gel loading buffer contained 2.5% (v/v) 2-ME. The samples were subsequently separated by SDS-PAGE.

Acknowledgments

The authors are grateful to Dr. Hanna Bramfeldt and Dr. Katarina Johansson for assistance with electron microscopy and mechanical testing.

References

1. Gosline JM, Guerette PA, Ortlepp CS, Savage KN (1999) The mechanical design of spider silks: from fibroin sequence to mechanical function. J Exp Biol 202:3295–3303.
2. Vollrath F, Knight DP (1999) Structure and function of the silk production pathway in the spider Nephila edulis. Int J Biol Macromol 24:243–249.
3. Sponner A, Unger E, Grosse F, Weisshart K (2005) Differential polymerization of the two main protein components of dragline silk during fibre spinning. Nat Mater 4: 772–775.
4. Rising A, Hjalm G, Engstrom W, Johansson J (2006) N-terminal nonrepetitive domain common to dragli flagelliform, and cylindriform spider silk proteins. Biomacromolecules 7:3120–3124.
5. Sponner A, Vater W, Rommerskirch W, Vollrath F, Unger E, Grosse F, Weisshart K (2005) The conserved C-termini contribute to the properties of spider silk fibroins. Biochem Biophys Res Commun 338:897–902.
6. Ittah S, Cohen S, Garty S, Cohn D, Gat U (2006) An essential role for the C-terminal domain of a dragline spider silk protein in directing fiber formation. Biomacromolecules 7:1790–1795.
7. Ittah S, Michaeli A, Goldblum A, Gat U (2007) A model for the structure of the C-terminal domain of dragline spider silk and the role of its conserved cysteine. Biomacromolecules 8:2768–2773.
8. Stark M, Grip S, Rising A, Hedhammar M, Engstrom W, Hjalm G, Johansson J (2007) Macroscopic fibers self-assembled from recombinant miniature spider silk proteins. Biomacromolecules 8:1695–1701.
9. Hedhammar M, Rising A, Grip S, Martinez AS, Nordling K, Casals C, Stark M, Johansson J (2008) Structural properties of recombinant nonrepetitive and repetitive parts of major ampullate spidroin 1 from *Euprosthenops australis*: implications for fiber formation. Biochemistry 47:3407–3417.
10. Seidel A, Liivak O, Calve S, Adaska J, Ji G, Yang Z, Grubb D, Zax DB, Jelinski LW (2000) Regenerated spider silk: processing, properties, and structure. Macromolecules 33:775–780.
11. Lazaris A, Arcidiacono S, Huang Y, Zhou J-F, Duguay F, Chretien N, Welsh EA, Soares JW, Karatzas CN (2002) Spider silk fibers spun from soluble recombinant silk produced in mammalian cells. Science 259:472–476.
12. Shao Z, Vollrath F, Yang Y, Thogersen HC (2003) Structure and behavior of regenerated spider silk. Macromolecules 36:1157–1161.
13. Vollrath F, Barth P, Basedow A, Engstrom W, List H (2002) Local tolerance to spider silks and protein polymers in vivo. In Vivo 16:229–234.
14. Allmeling C, Jokuszies A, Reimers K, Kall S, Vogt PM (2006) Use of spider silk fibres as an innovative material in a biocompatible artificial nerve conduit. J Cell Mol Med 10:770–777.
15. Yang Y, Chen X, Ding F, Zhang P, Liu J, Gu X (2007) Biocompatibility evaluation of silk fibroin with peripheral nerve tissues and cells in vitro. Biomaterials 28:1643–1652.
16. Kluge JA, Rabotyagova O, Leisk GG, Kaplan DL (2008) Spider silks and their applications. Trends Biotechnol 26: 244–251.
17. Wong Po Foo C, Patwardhan SV, Belton DJ, Kitchel B, Anastasiades D, Huang J, Naik RR, Perry CC, Kaplan DL (2006) Novel nanocomposites from spider silk-silica fusion (chimeric) proteins. Proc Natl Acad Sci USA 103: 9428–9433.
18. Cao B, Mao C (2007) Oriented nucleation of hydroxylapatite crystals on spider dragline silks. Langmuir 23: 10701–10705.
19. Huang J, Wong C, George A, Kaplan DL (2007) The effect of genetically engineered spider silk-dentin matrix protein 1 chimeric protein on hydroxyapatite nucleation. Biomaterials 28:2358–2367.
20. Allmeling C, Jokuszies A, Reimers K, Kall S, Choi CY, Brandes G, Kasper C, Scheper T, Guggenheim M, Vogt PM (2008) Spider silk fibres in artificial nerve constructs promote peripheral nerve regeneration. Cell Prolif 41: 408–420.
21. Ayoub NA, Garb JE, Tinghitella RM, Collin MA, Hayashi CY (2007) Blueprint for a high-performance biomaterial: full-length spider dragline silk genes. PLoS ONE 2:e514.

22. Vendrely C, Scheibel T (2007) Biotechnological production of spider-silk proteins enables new applications. Macromol Biosci 7:401–409.
23. Blackledge TA, Cardullo RA, Hayashi CY (2005) Polarized light microscopy, variability in spider silk diameters, and the mechanical characterization of spider silk. Invert Biol 124:165–173.
24. Fahnestock SR (1994) Novel, recombinantly produced spider silk analogs. Int. Application no. PCT/US94/06689, Int. Publication no. WO 94/29450.
25. Lewis RV, Hinman M, Kothakota S, Fournier MJ (1996) Expression and purification of a spider silk protein: a new strategy for producing repetitive proteins. Protein Expr Purif 7:400–406.
26. Arcidiacono S, Mello CM, Butler M, Welsh E, Soares JW, Allen A, Ziegler D, Laue T, Chase S (2002) Aqueous processing and fiber spinning of recombinant spider silks. Macromolecules 35:1262–1266.
27. Teulé F, Furin WA, Cooper AR, Duncan JR, Lewis RV (2007) Modifications of spider silk sequences in an attempt to control the mechanical properties of the synthetic fibers. J Mater Sci 42:8974–8985.
28. Bogush VG, Sokolova OS, Davydova LI, Klinov DV, Sidoruk KV, Esipova NG, Neretina TV, Orchanskyi IA, Makeev VY, Tumanyan VG, Shaitan KV, Debabov VG, Kirpichnikov MP (2008) A novel model system for design of biomaterials based on recombinant analogs of spider silk proteins. J Neuroimmune Pharmacol 17–27.
29. Brooks AE, Stricker SM, Joshi SB, Kamerzell TJ, Middaugh CR, Lewis RV (2008) Properties of synthetic spider silk fibers based on Argiope aurantia MaSp2. Biomacromolecules 9:1506–1510.
30. Zhou S, Peng H, Yu X, Zheng X, Cui W, Zhang Z, Li X, Wang J, Weng J, Jia W, Li F (2008) Preparation and characterization of a novel electrospun spider silk fibroin/poly(D,L-lactide) composite fiber. J Phys Chem B 112:11209–11216.
31. Vollrath F, Knight DP (2001) Liquid crystalline spinning of spider silk. Nature 410:541–548.
32. Winkler S, Szela S, Avtges P, Valluzzi R, Kirschner DA, Kaplan D (1999) Designing recombinant spider silk proteins to control assembly. Int J Biol Macromol 24:265–270.
33. Szela S, Avtges P, Valluzzi R, Winkler S, Wilson D, Kirschner D, Kaplan DL (2000) Reduction-oxidation control of beta-sheet assembly in genetically engineered silk. Biomacromolecules 1:534–542.
34. Winkler S, Wilson D, Kaplan DL (2000) Controlling beta-sheet assembly in genetically engineered silk by enzymatic phosphorylation/dephosphorylation. Biochemistry 39:12739–12746.
35. Hardy JG, Romer LM, Scheibel T (2008) Polymeric materials based on silk proteins. Polymer 29:4309–4327.
36. Gosline JM, DeMont EM, Denny MW (1986) The structure and properties of spider silk. Endeavour 10:37–43.
37. Termonia Y (1994) Molecular modeling of spider silk elasticity. Macromolecules 27:7378–7381.
38. O'Brien JP, Fahnestock SR, Termonia Y, Gardner KCH (1998) Nylons from nature: synthetic analogs to spider silk. Adv Mater 10:1185–1195.
39. Perez-Rigueiro J, Elices M, Llorca J, Viney C (2001) Tensile properties of Attacus atlas silk submerged in liquid media. J Appl Polym Sci 82:53–62.
40. Garrido MA, Elices M, Viney C, Perez-Rigueiro J (2002) The variability and interdependence of spider drag line tensile properties. Polymer 43:4495–4502.
41. Garrido MA, Elices M, Viney C, Perez-Rigueiro J (2002) Active control of spider silk strength: comparison of drag line spun on vertical and horizontal surfaces. Polymer 43: 1537–1540.
42. Perez-Rigueiro J, Elices M, Plaza G, Real JI, Guinea GV (2005) The effect of spinning forces on spider silk properties. J Exp Biol 208:2633–2639.
43. Du N, Liu XY, Narayanan J, Li LA, Lim MLM, Li DQ (2006) Design of superior spider silk: from nanostructure to mechanical properties. Biophys J 91:4528–4535.
44. Madsen B, Shao ZZ, Vollrath F (1999) Variability in the mechanical properties of spider silks on three levels: interspecific, intraspecific and intraindividual. Int J Biol Macromol 24:301–306.
45. Poza P, Perez-Rigueiro J, Elices M, Llorca J (2002) Fractographic analysis of silkworm and spider silk. Eng Fract Mech 69:1035–1048.
46. Liu Y, Shao Z, Vollrath F (2005) Relationships between supercontraction and mechanical properties of spider silk. Nat Mater 4:901–905.
47. Guinea GV, Perez-Rigueiro J, Plaza GR, Elices M (2006) Volume constancy during stretching of spider silk. Biomacromolecules 7:2173–2177.
48. Termonia Y, Smith P (1987) Kinetic-model for tensile deformation of polymers. I. Effect of molecular-weight. Macromolecules 20:835–838.
49. Termonia Y, Smith P (1988) Kinetic-model for tensile deformation of polymers. II. Effect of entanglement spacing. Macromolecules 21:2184–2189.
50. Challis RJ, Goodacre SL, Hewitt GM (2006) Evolution of spider silks: conservation and diversification of the C-terminus. Insect Mol Biol 15:45–56.
51. Sponner A, Unger E, Grosse F, Weisshart K (2004) Conserved C-termini of Spidroins are secreted by the major ampullate glands and retained in the silk thread. Biomacromolecules 5:840–845.
52. Clark ED (2001) Protein refolding for industrial processes. Curr Opin Biotechnol 12:202–207.
53. Wang SSS, Chang CK, Peng MJ, Liu HS (2006) Effect of glutathione redox system on lysozyme refolding in size exclusion chromatography. Food Bioprod Proc 84:18–27.
54. Guhrs KH, Weisshart K, Grosse F (2000) Lessons from nature—protein fibers. J Biotechnol 74:121–134.
55. O'Donnell IJ, Frangione B, Porter RR (1970) The disulphide bonds of the heavy chain of rabbit immunoglobulin G. Biochem J 116:261–268.
56. Park SH, Kim HE, Kim CM, Yun HJ, Choi EC, Lee BJ (2002) Role of proline, cysteine and a disulphide bridge in the structure and activity of the anti-microbial peptide gaegurin 5. Biochem J 368:171–182.
57. Wolfram LJ (1965) Reactivity of disulfide bonds in strained keratin. Nature 206:304–305.
58. Hu X, Kohler K, Falick AM, Moore AM, Jones PR, Vierra C (2006) Spider egg case core fibers: trimeric complexes assembled from TuSp1, ECP-1, and ECP-2. Biochemistry 45:3506–3516.
59. Hu X, Kohler K, Falick AM, Moore AM, Jones PR, Sparkman OD, Vierra C (2005) Egg case protein-1. A new class of silk proteins with fibroin-like properties from the spider Latrodectus hesperus. J Biol Chem 280:21220–21230.
60. Wellman SE, Case ST (1989) Disassembly and reassembly in vitro of complexes of secretory proteins from Chironomus tentans salivary glands. J Biol Chem 264:10878–10883.
61. Andersen SO (1964) The cross-links in resilin identified as Dityrosine and Trityrosine. Biochim Biophys Acta 93:213–215.
62. Lassandro F, Sebastiano M, Zei F, Bazzicalupo P (1994) The role of dityrosine formation in the crosslinking of CUT-2, the product of a second cuticlin gene of Caenorhabditis elegans. Mol Biochem Parasitol 65:147–159.
63. Andersen SO (2004) Regional differences in degree of resilin cross-linking in the desert locust, Schistocerca gregaria. Insect Biochem Mol Biol 34:459–466.